Potential for Novel Magnetic Structures by Nanowire Growth Mechanisms

R. R. LaPierre* and M. C. Plante

Centre for Electrophotonic Materials and Devices, Department of Engineering Physics, McMaster University, Hamilton, Ontario, L8S 4L7, Canada

GaAs nanowires were grown on GaAs (1 1 1)B substrates in a gas source molecular beam epitaxy system, using self-assembled Au particles with diameters between 25 and 200 nm as the catalytic agents. The growth rate and structure of the nanowires were investigated for substrate temperatures between 500 and 600 °C to study the mass transport mechanisms that drive the growth of these crystals. The possibilities for fabrication of novel magnetic nanostructures by suitable choice of growth conditions are discussed.

Key words : Nanowires, Molecular beam epitaxy, Gallium arsenide

1. Introduction

Magnetic nanowires, such as Mn:ZnO [1] and Mn:GaN [2, 3], are being explored for their applications in biology, spintronics, and data storage. Nanowires can be synthesized by a wide range of methods, including lithography [4], selective area epitaxy [5, 6] and electrochemical template synthesis [7], but bottom-up approaches that rely on the catalytic effect of a metal seed particle are probably the most promising for atomic scale control of device dimensions. Catalytic growth mechanisms include the vapor-liquid-solid (VLS) growth mechanism first proposed by Wagner and coworkers [8] more than 40 years ago to describe the growth of Si whiskers, as well as more recent variants such as the solution-liquid-solid (SLS) [9], and the vapor-solid-solid (VSS) [10, 11] mechanisms. In the case of III-V nanowires, various growth techniques have been used for catalytic growth, including metal-organic vapor phase epitaxy (MOVPE) [12, 13], molecular beam epitaxy (MBE) [14, 15], chemical beam epitaxy (CBE) [16], and laser-assisted growth [17]. As demonstrated in this work, these approaches offer the possibility of producing complex axial and radial heterostructures, which may exhibit novel magnetic transport properties that remain largely unexplored in the experimental domain [18]. In this article, we report GaAs nanowires grown by gas source

molecular beam epitaxy under different growth conditions and discuss the potential for fabricating novel magnetic nanostructures.

2. Experimental Details

Substrates of GaAs (1 1 1)B were first submitted to a 20-minute uv-ozone treatment in order to remove any contamination from hydrocarbons, and grow a sacrificial layer of oxide. After etching in a 10% buffered HF solution for 30 seconds and rinsing with deionized water, the samples were transported in ambient air to an e-beam evaporation system, where a 4.5 nm-thick film of Au was deposited as measured by a quartz crystal thickness monitor. The samples with Au deposit were then transferred in ambient air to the gas source molecular beam epitaxy (GS-MBE) growth chamber. In the GS-MBE system, group III species are supplied as monomers from a heated solid elemental source, and the group V species are supplied as dimers (As_2) from a hydride (AsH_3) gas cracker operating at 1000 °C. Prior to nanowire growth, the Au-covered substrates were heated to a temperature of 600 °C for 5 minutes under an As_2 flux in order to form Au-Ga alloyed nanoparticles on the surface. Simultaneous desorption of the GaAs native oxide was enhanced by the use of a hydrogen electron cyclotron resonance (ECR) plasma source, resulting in a total hydrogen pressure of about 1×10^{-4} Torr in the chamber. The temperature of the substrate was subsequently set to the desired value, and the Ga shutter opened to initiate the growth at a

*Corresponding author: Tel: +1-905-525-9140 (x27764), Fax: +1-905-527-8409, e-mail: lapierr@mcmaster.ca

nominal 2-D rate of 1 micron/hour for 30 minutes. Three growths were carried out at substrate temperatures of 500, 550, and 600 °C, and with a constant V/III flux ratio of 1.5.

After the growths, all samples were characterized using a field emission scanning electron microscope (SEM) in the secondary electron mode. Statistical data on surface density of catalysts and wires, catalyst diameter, wire height and wire diameter were obtained by measuring up to 550 catalysts and wires directly from the SEM images. The reported heights represent the visible part of the wires, above a 2-D growth layer that grew simultaneously on the parts of the surface not covered by Au particles. The measured heights of the wires were corrected to account for any sample tilt present during the SEM imaging.

3. Results

Tilted and top views of the post-growth surfaces are shown in Figure 1 a–f. All the wires grew normal to the surface, along the [1 1 1] direction, which is the preferred growth direction for GaAs nanowires [19]. The presence of Au at the end of the nanowires was confirmed by energy dispersive x-ray spectrometry, verifying that the wires grew by a catalytic process. The total wire densities were measured to be 8.5×10^8, 8.8×10^8, and 1.7×10^8 cm^{-2} for growth temperatures of 500, 550, and 600 °C, respectively. The significant difference between the density observed at 600 °C and the two lower temperatures

can be attributed to the coalescence of the self-assembled Au particles on the substrate before growth is initiated.

At low temperature (500 °C) the wires are tapered, which is most evident for catalyst diameters below ~100 nm. When the temperature is raised to 550 °C or above, the tapering vanishes, resulting in wires that have a filamentary shape with nearly uniform diameter along their entire length. Roughness of the surface surrounding each wire was observed, indicating that 2-D growth occurred simultaneously with the catalytic process on the Au covered areas. This last assertion was supported by cross-sectional SEM imaging of the growth samples using the focused ion beam (FIB) technique. Note that a similar 2-D layer was also observed and characterized using transmission electron microscopy (TEM) by Schubert and coworkers in the case of MBE-grown Si nanowires [20].

The height h of the nanowires was measured, and plotted as a function of the catalyst diameter d, for the three temperatures in Figure 2. To minimize crowding in the figure, the value of d represents the average of measurements within a 6 nm range, and the value of h is the average of the height measurements within that range. The error bars correspond to the standard deviation of h. A fitting on a log-log plot of the data in that region of the curve (not shown) indicates a clear $1/d$ dependence of the wire height, which has been observed and predicted by a number of previous groups, and has been attributed to diffusion of adatoms from the surface to the tops of the wires [20-22].

From the plan view images in Figure 1d–f, it is clear,
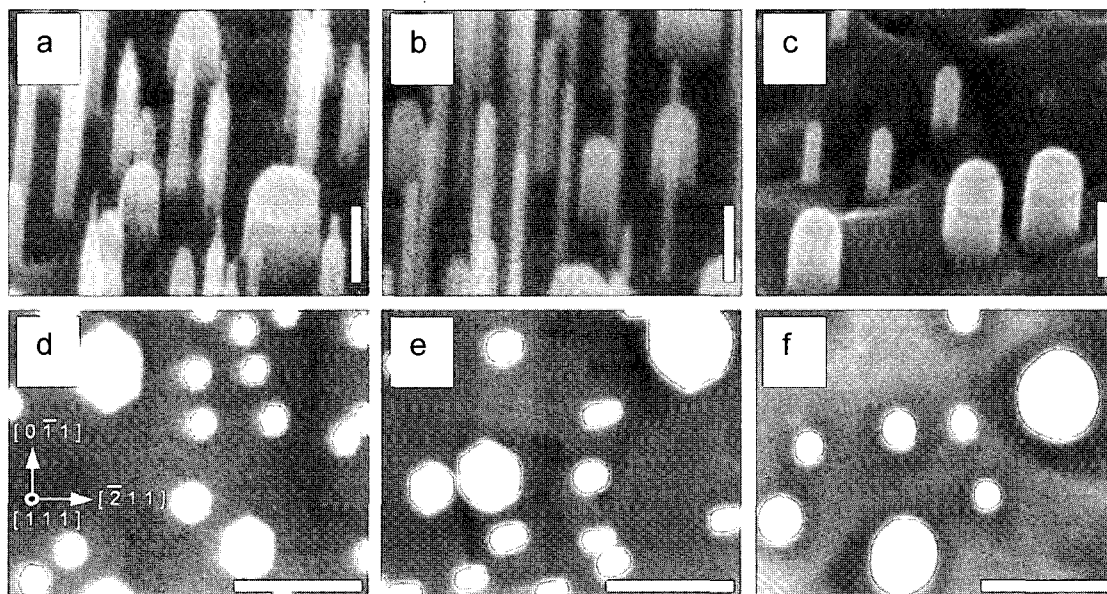
Fig. 1. 40° tilted (a – c) and top view (d – f) SEM images of Au-catalyzed GaAs nanowires grown at temperatures of: (a, d) 500 °C, (b, e) 550 °C, and (c, f) 600 °C. The length bars indicate 500 nm; the axes indicating the crystalline orientation in (d) are the same for (e, f).
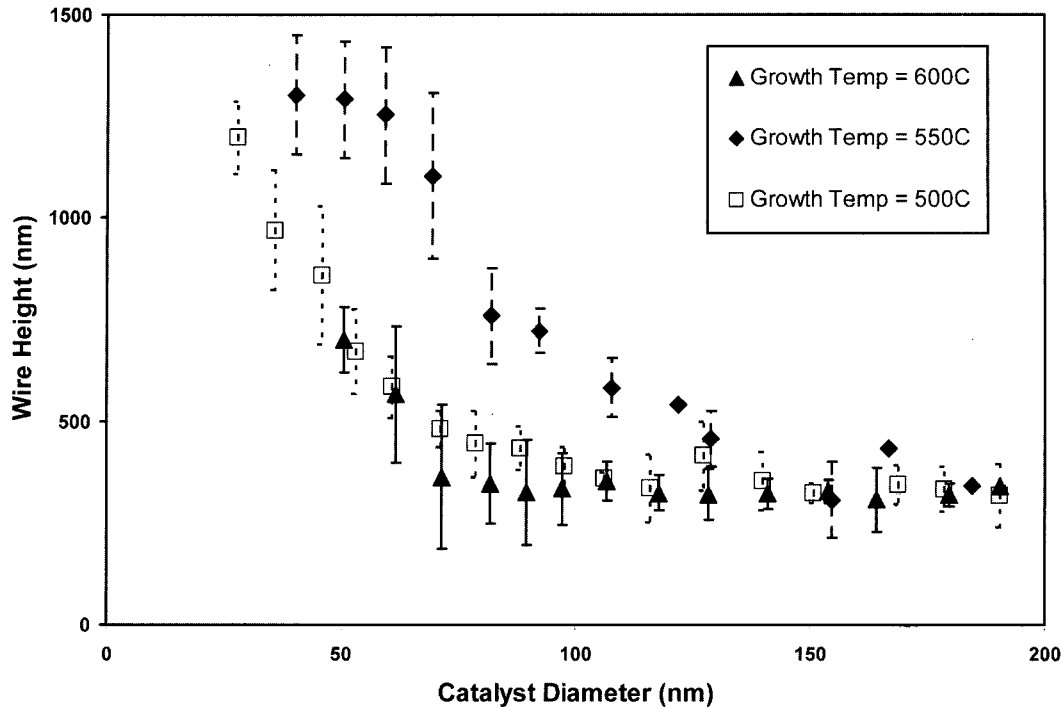
Fig. 2. Height of GaAs nanowires as a function of the catalyst diameter for growth temperatures of 500, 550, and 600 °C.

especially in the case of the 500 °C growth, that two different wire facets are observed. For d less than about 50 nm {–1 1 0} side walls were typically observed, while for larger catalyst diameters ($d > 50$ nm) {–2 1 1} facets were typically observed. In the case of 550 °C growth similar faceting is observed (transition between the two types occurring for $d \sim 70$ nm), while it has almost disappeared at 600 °C.

4. Discussion

The wire growth may be sustained by the mass transport of materials supplied via three pathways, as Bhunia and coworkers tabled in the case of MOVPE growth of InP nanowires [23], and as shown in Figure 3: (i) direct impingement of the growth species on the catalyst, then diffusion on its surface in a "random walk" manner until they reach the growth interface; (ii) direct impingement of the growth species on the catalyst followed by bulk diffusion through the Au; and (iii) a "random walk" diffusion of the adatoms on the 2D substrate surface at the base of the wires then along the wire sidewalls up to the growth interface. In the case of (i) and (iii), incorporation into the wire crystal is accomplished via diffusion along the catalyst-wire interface as described elsewhere [24]. Pathways (i) and (ii) (i.e. direct impingement on the catalyst) yield a

constant growth rate that is independent of the catalyst size. As this does not correspond to what is experimentally observed, the substrate surface diffusion must be considered the main contributor in the initial stages of wire growth. We already pointed out in the previous section that the $1/d$ dependence of h (see Figure 2) is a typical signature of this mechanism. In other studies of III-V nanowires grown by CBE [16] and MBE [22] though, the group V diffusion is neglected (e.g. group V supply is limited to direct impingement). It is however worth noticing that the conditions that prevailed during our growths (V/III flux ratio of 1.5, nominal 2-D rate of 1 μm/h, duration of 30 minutes) imply that there is enough As for wires up to 750 nm high (= 1 μm/h × 30 minutes × 1.5), if only direct impingement on the catalyst is considered. However, wires that were almost twice as tall as this limit were measured, leading us to conclude that path (iii) cannot be completely ruled out for group V species. Also, desorption of As_2 from the 2-D surface, followed by impingement on the wire sidewalls, may constitute an additional source of group V materials that sustains the wire growth.

The absence of tapering, coupled with the observation of optimum growth rate, at a temperature of 550 °C leads to the conclusion that Ga adatoms impinging on the 2-D surface under these conditions may optimally diffuse up the wire to reach the growth interface. When the growth
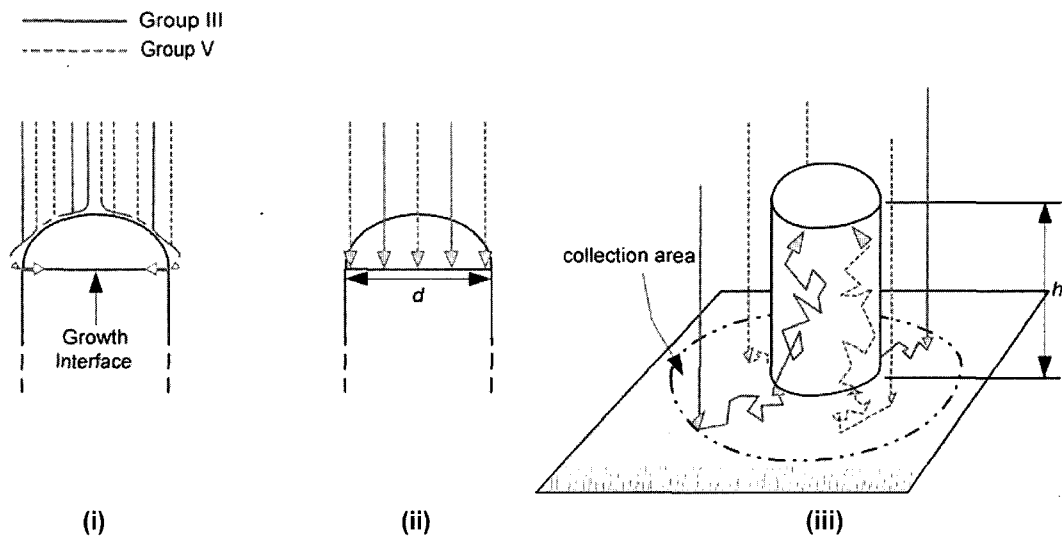
Fig. 3. Mechanisms for the GS-MBE growth of III-V nanowires. Materials are supplied to the growth interface via: (i) direct impingement of the growth species on the catalyst, then diffusion on its surface; (ii) direct impingement of the growth species on the catalyst followed by bulk diffusion through the Au; (iii) diffusion of the growth species on the 2D surface then along the wire sidewalls, in a "random walk" manner. For (i) and (iii) the species incorporate in the crystal by diffusion along the Au-wire interface.

temperature is lowered (e.g. 500 °C), the adatom diffusivities are less thus resulting in shorter diffusion lengths. It is thus suggested that the species do not reach the wire growth interface, and instead find nucleation sites on the sidewalls, which results in the tapering (or radial growth) observed experimentally (Figure 1a). While similar morphology has been reported in previous studies [16], the exact nature of this tapering is however still not fully understood, and additional experiments and theoretical work are needed to clarify the mass transport mechanisms involved. When the temperature is raised (e.g. 600 °C), the diffusivities are greater but the adatoms have shorter surface residency times and therefore a greater probability of desorbing before reaching the Au catalyst, again resulting in shorter wires.

The difference in sidewall faceting observed for catalyst diameter above and below 70 nm (for growth at 550 °C)

or 50 nm (for growth at 500 °C) probably has its origin in the crystalline structure of the wires. For instance, Persson and coworkers in their CBE growth study [16] identified the {-1 1 0} facets with the zincblende crystal structure. It is then possible that the observed {-2 1 1} facets could actually be the {-1 1 2 0} surfaces of the wurtzite structure. For nanowires with diameters around the transition value, the faceting was not as obvious, and the wire cross-sections appeared almost circular. This is believed to be the result of alternating layers of the two crystal structures (i.e. zincblende and wurtzite intermixed due to a rotating twin at every (1 1 1) plane of the zincblende structure, as proposed by Hiruma and coworkers [19]).

Tailoring of the diameter, aspect ratio, and topology of nanowires enables the tuning of their magnetic properties [25]. For example, it is possible to modulate the composi-
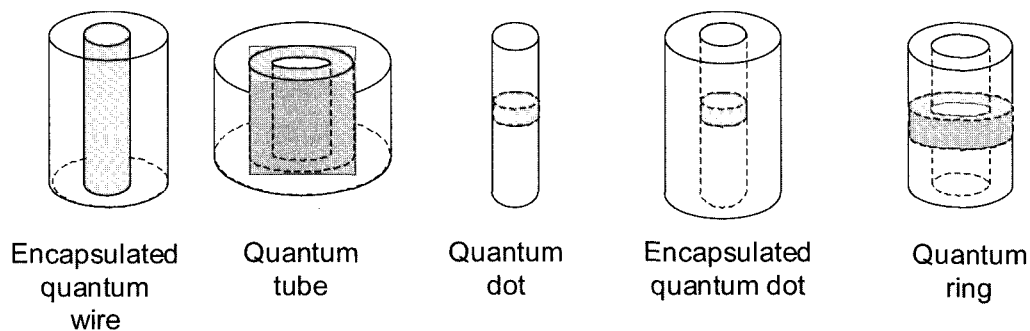
Fig. 4. Potential quantum structures expected from the variation of MBE growth conditions.

tion and doping along the length of nanowires with atomic-scale precision by switching of the molecular beams during growth. The change in wire structure (tapered versus filamentary) with growth temperature opens the possibility of creating complex radial and axial growth structures as depicted in Figure 4. For example, core-shell quantum structures may be achieved by growth of uniform diameter wires of a low bandgap material at a particular temperature (550 °C for GaAs), followed by growth of a higher bandgap material at lower temperature leading to encapsulation. Combining these approaches may produce heterostructures of varying topology such as quantum dots and rings. Dilute magnetic semiconductors in these unique topologies remains a largely unexplored field. For example, a quantum ring surrounding a dilute magnetic nanowire core could yield unique magneto-optic and transport properties [18].

5. Conclusions

The GS-MBE growth of GaAs nanowires on GaAs (1 1 1)B surfaces has been investigated as a function of the temperature and the size of the Au seed particle. The experimental observations indicated that crystal growth was sustained by diffusion of Ga adatoms on the 2-D surface and along the crystal sidewalls up to the growth interface. The average wire growth rate exceeded the limit expected from the V/III flux ratio, suggesting that group V species reach the growth interface via a combination of desorption from the 2-D surface and diffusion on the wire sidewalls.

Two distinct growth regimes, with different crystal structures were observed when the size of the catalyst was varied around 100 nm. Further SEM and transmission electron microscopy analysis of the wires are currently in progress to elucidate these growth mechanisms. The potential for magnetic nanostructures was presented.

Acknowledgements

References

[1] Y. W. Heo, D. P. Norton, L. C. Tien, Y. Kwon, B. S. Kang, F. Ren, S. J. Pearton, and J. R. LaRoche, Mat. Sci. Eng. R **47**, 1 (2004).

[2] H.-J. Choi, H.-K. Seong, J. Chang, K.-I. Lee, Y.-J. Park, J.-J. Kim, S.-K. Lee, R. He, T. Kuykendall, and P. Yang, Adv. Mater. **17**, 1351 (2005).

[3] J. M. Baik and J.-L. Lee, J. Vac. Sci. Technol. B **23**(2), 530 (2005).

[4] Y. Sun, D.-Y. Khang, F. Hua, K. Hurley, R. G. Nuzzo, and J. A. Rogers, Adv. Funct. Mater. **15**, 30 (2005).

[5] J. Motohisa, J. Noborisaka, J. Takeda, M. Inari, and T. Fukui, J. Cryst. Growth **272**, 180 (2004).

[6] S. Yoshida, I. Tamai, T. Sato, and H. Hasegawa, Jpn. J. Appl. Phys. **43**, 2064 (2004).

[7] J. C. Hulteen and C. R. Martin, J. Mat. Chem. 7(7), 1075 (1997).

[8] R. S. Wagner, in: A. P. Levitt (Ed.), Whisker Technology, Wiley Inter-Science, New York (1970) pp. 47-119.

[9] T. J. Trentler, K. M. Hickman, S. C. Goel, A. M. Viano, P. C. Gibbons, and W. E. Buhro, Science **270**, 1791 (1995).

[10] T. I. Kamins, R. S. Williams, D. P. Basile, T. Hesjedal, and J. S. Harris, J. Appl. Phys. **89**, 1008 (2001).

[11] A. I. Persson, M. W. Larsson, S. Stenström, B. J. Ohlsson, L. Samuelson, and L. R. Wallenberg, Nature Mat. 3, 677 (2004).

[12] K. Hiruma, M. Yazawa, T. Katsuyama, K. Ogawa, K. Haraguchi, and M. Koguchi, J. Appl. Phys. 77, 447 (1995).

[13] M. Borgström, K. Deppert, and L. Samuelson, J. Cryst. Growth **260**, 211 (2004).

[14] V. G. Dubrovskii, I. P. Soshnikov, G. E. Cirlin, A. A. Tonkikh, Y. B. Samsonenko, N. V. Sibirev, and V. M. Ustinov, Phys. Stat. Sol B **241**, R30 (2004).

[15] Z. H. Wu, M. Sun, X. Y. Mei, and H. E. Ruda, Appl. Phys. Lett. **85**, 657 (2004).

[16] A. I. Persson, B. J. Ohlsson, S. Jeppesen, and L. Samuelson, J. Cryst. Growth **272**, 167 (2004).

[17] X. Duan and C. M. Lieber, Adv. Mater. **12**, 298 (2000).

[18] V. Gudmundsson, Y.-Y. Lin, C.-S. Tang, V. Moldoveanu, J. H. Bardarson, and A. Manolescu, Phys. Rev. B **71**, 235302 (2005).

[19] K. Hiruma, M. Yazawa, K. Haraguchi, K. Ogawa, T. Katsuyama, M. Koguchi, and H. Kakibayashi, J. Appl. Phys. **74**, 3162 (1993).

[20] L. Schubert, P. Werner, N. D. Zakharov, G. Gerth, F. M. Kolb, L. Long, U. Gösele, and T. Y. Tan, Appl. Phys. Lett. 84(24), 4968 (2004).

[21] V. Ruth and J. P. Hirth, J. Chem. Phys. 41(10), 3139 (1964).

[22] V. G. Dubrovskii, G. E. Cirlin, I. P. Soshnikov, A. A. Tonkikh, N. V. Sibirev, Y. B. Samsonenko, and V. M. Ustinov, Phys. Rev. B **71**, 205325 (2005).

[23] S. Bhunia, T. Kawamura, S. Fujikawa, and Y. Watanabe, Physica E **24**, 138 (2004).

[24] H. Wang and G. S. Fischman, J. Appl. Phys. **76**, 1557 (1994).

[25] L. Sun, Y. Hao, C.-L. Chien, and P. C. Searson, IBM J. Res. Dev. 49(1), 79 (2005).